

RESEARCH

Open Access

# Measurement of maize stalk shear moduli



Joseph Carter<sup>1</sup>, Joshua Hoffman<sup>1</sup>, Braxton Fjeldsted<sup>1</sup>, Grant Ogilvie<sup>1</sup> and Douglas D. Cook<sup>1,2\*</sup>

## Abstract

Maize is the most grown feed crop in the United States. Due to wind storms and other factors, 5% of maize falls over annually. The longitudinal shear modulus of maize stalk tissues is currently unreported and may have a significant influence on stalk failure. To better understand the causes of this phenomenon, maize stalk material properties need to be measured so that they can be used as material constants in computational models that provide detailed analysis of maize stalk failure. This study reports longitudinal shear modulus of maize stalk tissue through repeated torsion testing of dry and fully mature maize stalks. Measurements were focused on the two tissues found in maize stalks: the hard outer rind and the soft inner pith. Uncertainty analysis and comparison of multiple methodologies indicated that all measurements are subject to low error and bias. The results of this study will allow researchers to better understand maize stalk failure modes through computational modeling. This will allow researchers to prevent annual maize loss through later studies. This study also provides a methodology that could be used or adapted in the measurement of tissues from other plants such as sorghum, sugarcane, etc.

**Keywords** Biomechanics, Modeling, Torsion, Modulus, Shear

## Introduction

More maize is produced than any other crop in the world [26]. Maize is a major source for feeding livestock and has industrial applications in the production of ethanol and plastics. Maize and its byproducts can be found in almost every household. Because of this, any issue in the growth or harvest of maize has a long and lasting impact. One such problem is stalk lodging.

Stalk lodging is the breakage of maize stalks below the ear. This can lead to harvesting problems and can significantly impact crop yield. The failure process in stalk lodging is a complex process that depends on many factors, such as material properties [17], stalk morphology [23, 27], and loading direction. The most common tool for modeling this process is finite element modeling (FEA). FEA has been used to provide insights on the topic of

stalk lodging [17, 27], but the accuracy of these predictions is heavily influenced by our lack of knowledge of the many material constants of maize stalk tissue. A previous study has shown that uncertainty in material constants contributes greatly to the predictive accuracy of 3D parameterized maize stalk models in linear buckling analysis [17]. Therefore, it is of utmost importance that researchers quantify each of the material constants of maize stalks in order to better understand stalk lodging.

The motivation for this research was to better define the material properties for 3D parameterized FEA models developed by Ottesen et al [16]. These models are defined with transverse isotropic materials consisting of a pith and rind [22, 23, 27] and were created to better understand maize stalk failure modes and eventually increase crop yield [17].

Maize stalks contain two distinct materials, a hard outer shell (the rind) and a soft inner tissue (the pith). Both of these materials can be reasonably approximated as transversely isotropic [22, 23, 27]. The mechanical behavior of transversely isotropic materials is determined by six material properties. Five of these material properties are independent [5]. These six material properties

\*Correspondence:

Douglas D. Cook  
ddc971@byu.edu

<sup>1</sup> Brigham Young University, Provo, USA

<sup>2</sup> Department of Mechanical Engineering, Brigham Young University, Provo, UT 84602, USA



© The Author(s) 2024. **Open Access** This article is licensed under a Creative Commons Attribution-NonCommercial-NoDerivatives 4.0 International License, which permits any non-commercial use, sharing, distribution and reproduction in any medium or format, as long as you give appropriate credit to the original author(s) and the source, provide a link to the Creative Commons licence, and indicate if you modified the licensed material. You do not have permission under this licence to share adapted material derived from this article or parts of it. The images or other third party material in this article are included in the article's Creative Commons licence, unless indicated otherwise in a credit line to the material. If material is not included in the article's Creative Commons licence and your intended use is not permitted by statutory regulation or exceeds the permitted use, you will need to obtain permission directly from the copyright holder. To view a copy of this licence, visit <http://creativecommons.org/licenses/by-nc-nd/4.0/>.

are listed in Table 1. When analyzing maize stalks (which are composed of two transversely isotropic materials: the pith and the rind), twelve (ten independent) material properties are needed to model their behavior. Because of the difficulties in measuring maize stalk tissues materials (e.g. asymmetrical geometry and variation in specimens), research on maize stalk material properties has been relatively limited.

Although data regarding maize stalk properties are scarce, some of the twelve material properties have been measured previously. The longitudinal modulus of rind tissue is the most commonly reported maize tissue property [1, 2, 29, 30]. This is because the longitudinal rind modulus is relatively simple to measure and it has been shown to be influential in failure modeling [17].

The longitudinal modulus of pith tissue is more difficult to measure due to its low stiffness and fragility. Studies often adopt an inference-based approach to measure this property—a researcher will measure material response of an intact specimen (pith and rind), remove the pith, test the specimen again (with just the rind), and infer the contribution of the pith. Sutherland [25], Zhang [30], and Al-Zube [1] have reported the longitudinal modulus of elasticity of pith tissues.

The transverse modulus of pith and rind tissue is also difficult to measure. This is because there are no closed form equations to calculate modulus values for transverse compression testing (as opposed to three point bending or simple tension testing). Stubbs et al. used an inverse-FEA process in order to calculate the transverse modulus of elasticity of maize pith and rind tissues [23, 24].

For late-season stalk lodging, researchers are most interested in tissue properties at the time of harvest when stalks often have a relatively low moisture content. As a result, tissues are often classified as “dry” (moisture content below 15%) or “wet” (moisture content above 15%). Dry tissues are most relevant to late-season stalk lodging

[20] while wet tissue properties are more relevant to mid-season stalk lodging or greensnap [25]. Dry tissues have the advantage of being more amenable to laboratory testing since they are much more stable and easier to test than wet tissues. In general, tissue stiffness is highest for dry tissues and decreases as moisture content increases [25, 29, 30].

While many properties have been measured, several remain unmeasured. The properties that have not yet been measured include poisson’s ratios and shear modulus values. These properties are either difficult to measure or are believed to have a less significant influence on material response in maize stalks [17]. Of these remaining material properties, the longitudinal shear modulus of pith and rind tissue is the easiest to measure. This is because shear modulus is most often measured through torsion testing, and it is relatively easy to grip a maize stalk along its fibers (in the longitudinal direction). Table 1 summarizes the maize stalk tissue properties that have and have not been measured and shows how this study fills a gap in our understanding of maize stalk tissue properties.

The goal of this research was to measure the longitudinal shear modulus of dried maize stalk pith and rind tissues so that future studies that require these properties can be based upon empirical data instead of estimates, as has been necessary in the past [17] (Stubbs et al. 31). In particular, measurements were taken only on dried maize stalk samples for two reasons: first, dried stalks are easier to measure than wet ones, and second, because we are most concerned with stalk behavior at the time of harvest, when stalks are relatively dry [20, 25] (Stubbs et al. 31). Through this research, a 95% confidence level distribution of pith and rind longitudinal shear moduli was developed. This knowledge will be used to improve computational models of maize stalks, thereby enabling a better understanding of the mechanisms involved in stalk lodging.

**Table 1** summary of which maize stalk tissue properties have and have not been measured, including whether measurements were included for both wet and dry specimens

Source	$E_{  }$	$E_{\perp}$	$G_{  }$	$G_{\perp}$	$\nu_{  }$	$\nu_{\perp}$	Pith	Rind	Wet	Dry
Al-Zube et al. 2017	✓							✓		✓
[2]	✓							✓		✓
[24]		✓					✓	✓		✓
Stubbs et al. 2020		✓					✓	✓		✓
[25]	✓						✓	✓	✓	✓
Zhang et al. 2017	✓						✓		✓	✓
Zhang et al. 2016	✓							✓	✓	✓
Present study			✓				✓	✓		✓

## Methods

### Overview

Torsion tests were performed on dried maize stalks by twisting specimens as shown in Fig. 1. Specimens were gripped at nodes to prevent crushing due to the gripping pressure. The applied torque and rotation were measured simultaneously during each test. Following each test, the geometry of the stalk was quantified. Finally, the shear modulus was calculated based on the torque/rotation slope and the geometry of the specimen. The following sections describe the theoretical basis for this approach as well as the experimental methods that were utilized.

The general approach used in this study is very similar to well established methods for measuring similar materials [4]. Such torsion tests were conducted on dried bamboo [3, 12, 19] and 10–12% moisture content wood [6, 9]. Because we measured our tissues at 10–15% moisture content, it is reasonable to compare our measurements to both Moran and Green.

### Theory

The shear modulus,  $G$ , is a measure of a material’s resistance to shear deformation. For a prismatic 3D member, the equation relating shear deformation,  $\theta$ , to applied torque,  $T$ , is:

$$\theta = \frac{TL}{GK} \tag{1}$$

Here  $L$  represents the length over which the torque is applied and  $K$  is the torsional constant, a factor that accounts for the cross-sectional geometry of the object [7]. This equation can be solved for the shear modulus:

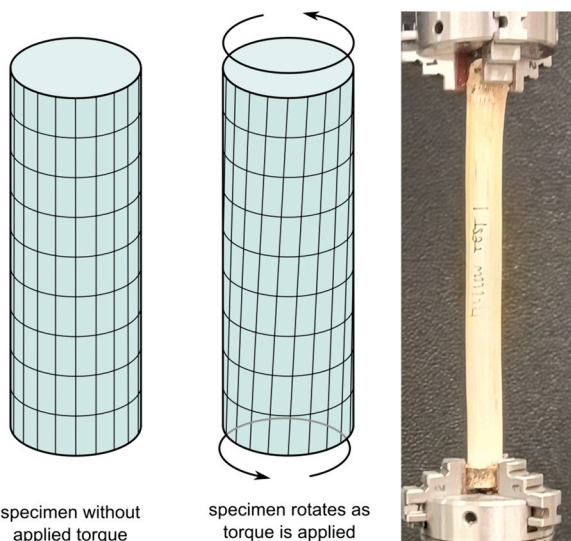


**Fig. 1** Torsion testing illustration and photograph of experimental set up

$$G = \frac{T L}{\theta K} \tag{2}$$

For a circular section, this simplifies to the more familiar form  $\frac{TL}{J\theta}$  where  $J$  is the polar area moment of inertia. However, for a specimen of *arbitrary* cross section (as for a maize stalk), the torsional constant should be used [5, 18].

The theory described above relies upon several assumptions. First, the theory assumes that the member subjected to torsion is prismatic. Second, the theory assumes that the tissue is linearly elastic with small levels of deformation. These assumptions are discussed below.

“Prismatic” means that the cross section of a specimen is uniform along its length. While the cross-sectional shape of maize stalks is not perfectly uniform, there is very little change in the cross-sectional shape between nodes [20]. The nearly uniform shape of the maize stalk is shown in Fig. 2.

The assumption for small deformations in Eq. 2 is met so long as the angle of twist is small. To account for this, we twisted specimens by only a small amount—from 0 to 5 degrees. This approach kept measurements within the linear elastic region.

### Specimen groups and selection

Specimens for this study came from maize stalks that were grown in an open field in Spanish Fork Utah during the 2021–2022 growing seasons. Three different commercial varieties of maize were used for testing. However, since the purpose of this study was to report a range of feasible values for the longitudinal shear modulus of maize, the influence of variety was not used as an experimental factor in this study. Stalks were harvested once grain filling had completed and just before harvest. This time point corresponds to the period when late-season stalk lodging is most likely to occur [20]. The stalks were cut with pruning shears just above the root and immediately transferred to the lab for specimen preparation. Figure 2 shows a representative sample cutting location on an intact maize stalk.

Specimen dimensions were limited by the physical constraints of the torsion tester (MTS Acumen 12, Eden Prairie, MN). The maximum length of specimens was constrained to 20 cm and the maximum diameter of specimens was constrained to 2.5 cm. These limits excluded only a small number of very large diameter stalks. Cuts were made 2–3 cm above and below a node (see Fig. 2) so that miniature lathe chucks could grip the nodes, which are sturdier and easier to grip. Each specimen was inspected for disease, pest damage, cracks, or any other damage before being chosen. Any damaged specimens were excluded from testing.

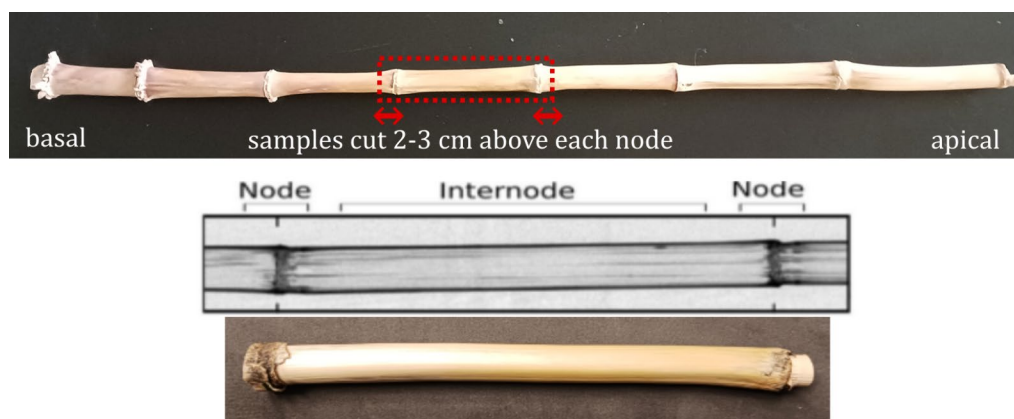


**Fig. 2** Example specimen location for sample selection. The specific location of a stalk was chosen based on whether the length was less than 20 cm and the diameter was less than 2.5 cm

Two different specimen groups were created in order to observe specific phenomena in testing: rind-only specimens (pith tissue removed), and pith-only specimens (rind tissue removed):

**Rind Only Specimens:** Specimens with only rind tissue were used to directly measure the shear modulus of the rind. To create rind-only specimens, the pith was carefully removed using drill bits, dissection spatulas, and abrasive pipe cleaners. Care was taken to ensure that the rind was not damaged in this process. If cracking occurred during pith removal, the specimen was not used. Due to the difficulty in preparing rind-only specimens, only 18 rind-only tests were performed.

**Pith Only Specimens:** Specimens with only pith tissue were used to directly measure the shear modulus of the pith. To create pith-only specimens, the rind was carefully removed using a razor blade. If cracking occurred during rind removal, the specimen was not used.

## Gripping specimens

### Method for gripping

Gripping specimens is always a challenge with biological tissues. If specimens are not gripped tightly enough, slipping may occur which adversely affects the collected data. On the other hand, if specimens are gripped too tightly, the specimen may be damaged. To mitigate these problems, 180 grit sandpaper was glued to the gripping jaws. This allowed the jaws to provide substantial gripping force which prevented slipping while also avoiding crushing or cracking the specimen. Tests were not performed if cracks occurred during the grip tightening phase. Because gripping involves multiple points of contact, the center of rotation can change slightly depending on how a specimen is gripped. To mitigate this effect and to account for other sources of random measurement

errors, each specimen was fixtured and tested using 3–5 replications of the torsion test.

### Torque/angle measurement

Both torque  $T$  and angle of twist  $\theta$  were measured by a 3 kip-MTS Acumen torsion/tensile testing device. The torque transducer for this device was a 662.30H-02B Model 30 N·m capacity transducer. The angle measurement for this device was a 494.47 Encoder B Rotary Encoder. Each specimen was loaded from 0 to 5 degrees at a rate of 0.15 degrees per second. This load speed was chosen because it was deemed slow enough to be considered static loading (viscoelastic effects could be neglected). Torque and angle were measured simultaneously during testing.

### Assessing slippage—alternative angle measurement

As stated previously, any shifting/slipping of the specimen during the torsion test will produce inaccuracies in the angle of twist measurement. Slipping can occur incrementally, making it very difficult to detect. To assess whether or not slippage of the grips was a problem, a second method for measuring the angle of twist was developed. This second method relied upon the rotation of two lasers attached directly to the specimen itself (see Fig. 3). Because there are no external loads applied to the lasers, this approach is not subject to any slippage.

Under the laser method, two Feyachi 9 mm bore sight lasers were attached at the outer thirds of each specimen as shown in Fig. 3. The lasers were aimed at a grid located a known distance from the specimen. A Nikon DSLR Z2 camera with a zoom lens was used to capture the location of the laser dots relative to the grid. During torsion testing, the lasers twisted with the maize stalks, and the

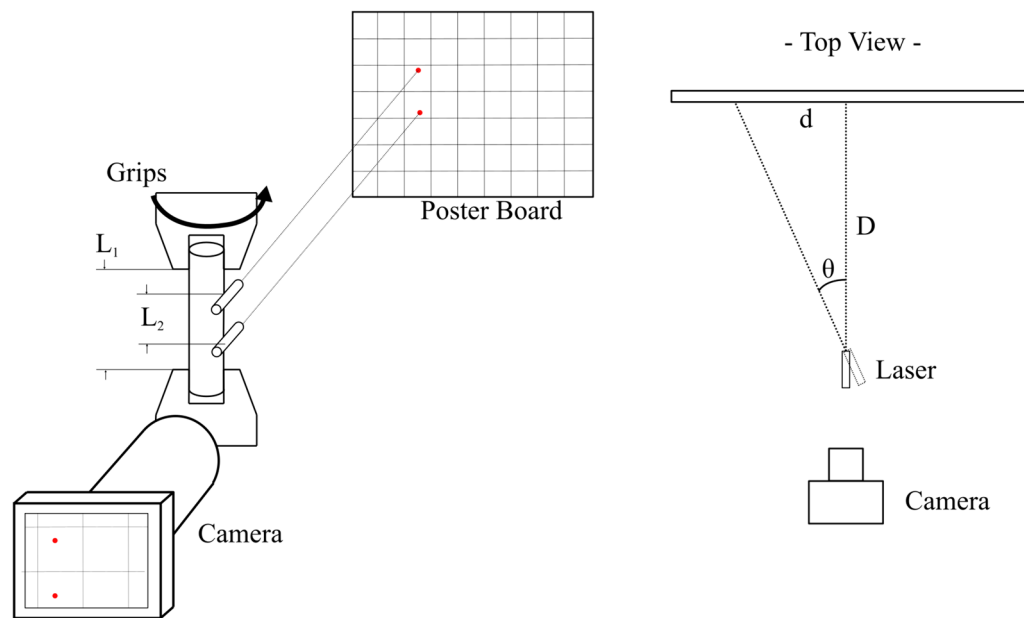


**Fig. 3** Laser setup. Left: two lasers were attached to the outer thirds of a specimen and pointed at a grid-poster board some distance away. A camera with a zoom lens tracked the movement of the laser dots over time.  $L_1$  was the grip length used in the torsional stiffness calculation for standard samples, and  $L_2$  was the grip length used in the torsional stiffness calculation for laser samples. Right: Trigonometry of camera setup. The angle  $\theta$  was calculated with  $\theta = \tan^{-1}[d/D]$ , where  $d$  was the position of the laser dot on the poster board and  $D$  was the distance from the laser to the poster board

paths of the laser dots were captured by a sequence of photographs.

To align the laser data with the torque and rotation data, the Nikon camera was triggered using an output signal from the torsion tester. Two photographs were taken every second during a torsion test (2 Hz sampling). As most tests took approximately 2 min to complete, this resulted in over 200 photographs per test. Each frame captured by the camera was analyzed using computer vision techniques to determine the position of each laser dot over time. Using trigonometry, the angle of twist between the two points was calculated over time, as shown in Fig. 3.

#### Comparing encoder rotation with laser rotation

Rotation was thus measured using two approaches: the rotations of the grips themselves as recorded by the rotary encoder (we call this the ‘rotary encoder’ measurement procedure), and the rotation as measured by the laser method described above (we call this the ‘laser’ measurement procedure). Any discrepancies between the two tests provided evidence of slippage. Because the length of specimen differed between grips and between lasers, the appropriate quantity for comparison between the rotary encoder data and the laser data was the torsional stiffness,  $GK$ , which is defined as:

$$GK = \frac{T}{\theta}L \quad (3)$$

where  $T$  was the torque measured by the MTS Acumen (identical in both tests);  $\theta$  was the angle of twist; and  $L$  was the length of the specimen for which twist was measured. These lengths are shown in Fig. 3 as  $L_1$  (for the standard measurement) and  $L_2$  for the laser measurement. A two sample  $t$ -test was used to compare results obtained using this laser measurement technique and those measured using the ‘standard’ angle measurement technique. Comparisons between the two methods for measuring rotation are presented in Sect. “Influence of slippage”.

#### Quantifying specimen geometry

##### Specimen length measurements

The effective length,  $L$ , of each specimen was measured. Before a torsion test began, a standard 1 mm precision flexible tape measure was used to measure the distance between the grips. This distance measurement was used for each subsequent test per specimen. Uncertainties in length measurements are explored in Sect. “Measurement uncertainty”.

### Specimen cross-sectional geometry

We used formulas from *Roark's Formulas for Stress and Strain* [7] to calculate  $K$  for both pith-only sections and rind-only sections. For pith-only cross sections, we used Roark's equation for arbitrary *solid* cross sections: [5, 7, 15]

$$K_{pith} = \frac{A_{pith}^2}{40J_{pith}} \quad (4)$$

where  $A_{pith}$  is the area encapsulated by the pith section and  $J_{pith}$  is the polar moment of the area of the pith section. For hollow rind-only cross sections, we used Roark's equation for arbitrary *thin walled* hollow cross sections: [5, 7, 15]

$$K_{rind} = \frac{4A_m^2}{\oint ds/t} \quad (5)$$

Here  $A_m$  was the area encapsulated by the thin wall midline,  $s$  was the distance along the midline, and  $t$  was a function of  $s$  along the midline.

The geometric information used in these equations was obtained from optical scans of specimen cross sections. Specimens were first cut perpendicular to their length with a bandsaw to expose the inner cross-section. These cross sections were held against an Epson Perfection V39 flatbed scanner and scanned at 2400 dpi. These images were then exported to MATLAB as JPEGs for image processing.

In MATLAB, the Visual Processing Toolbox's imageSegmenter function was used to create digital masks of each image. A region of interest tool was used to mark the relevant pixels for calculations. Figure 4 outlines various steps of this process.

### Uncertainty in measurements

It is important to consider the degree of uncertainty when reporting measured values of plant tissues [13]. In this study, three quantities were required to calculate shear modulus: the  $T/\theta$  slope,  $L$ , and  $K$ . Each of these quantities were subject to measurement uncertainty. In this paper, we will define the measurement uncertainty of all quantities as the two-sided 95% confidence interval of the mean measurement. This quantity is written as

$$u = t_{95, n-1} \frac{s}{\sqrt{n}} \quad (6)$$

where  $t_{95}$  was the 95% confidence t-statistic drawn from the student's t distribution with  $n - 1$  degrees of freedom,  $s$  was the sample standard deviation, and  $n$  was the number of measurements for a given specimen.

The quantity  $T/\theta$  was measured 3–5 times for each specimen with the MTS Acumen. The specimen was removed from the machine and refixed between each test. The standard deviation of these measurements was used in Eq. 6 to calculate  $u_{T/\theta}$  for each set of repeated specimen measurements. This uncertainty was unique for each specimen.

The quantity  $L$  was measured as the distance between the two grips for a specimen. This was measured with a standard 1 mm increment tape measure. To estimate the variation in measuring the length  $L$ , one sample was fixtured and measured 10 times by one user. The standard deviation of this repeated measurement was used with Eq. 6 to calculate an uncertainty that was applied to all samples.

The quantity  $K$  was measured through numerical integration of the formulas described in Sect. "Quantifying specimen geometry". The biggest source of error in this measurement came from variation in manually identifying the pixels in a cross section scan as being either pith pixels or rind pixels. Erroneously identifying pith pixels



**Fig. 4** Three steps of the image segmentation process. We first imported an image to MATLAB (left), then we separated the rind pixels from the pith pixels using the segmenter tool (middle), then relevant quantities were calculated using MATLAB functions (right)

as being rind pixels would inflate the  $K$  calculated for the rind while depressing the  $K$  value for the pith. To estimate the variation caused by the manual segmentation process, the torsional constant of one cross section scan was calculated 10 times by one user. The standard deviation of the resulting torsional constants was used with Eq. 6 to calculate a  $u_K$  that was applied to both pith-only and rind-only specimens.

**Propagation of uncertainty**

The Monte Carlo error propagation method [8] was used to determine the overall uncertainty in shear modulus. The mean and standard deviation values for  $T/\theta$ ,  $L$ , and  $K$  were calculated for each specimen. Normal distributions were then created for each quantity based on these respective mean and standard deviations. These distributions were then sampled 100 times for each quantity and combined to produce a distribution of corresponding  $G$  values. The mean  $G$  value was carried forward as the best estimate of  $G$  for each specimen. The standard deviation of the  $G$  distribution was used with Eq. 6 to calculate the propagated uncertainty in shear modulus,  $u_G$ .

It is often easier to visualize uncertainties in terms of percent uncertainty. The percent uncertainty for any of the quantities discussed above can be calculated with Eq. 7:

$$u_{\%} = (u/) \times 100\% \tag{7}$$

where  $u$  was the uncertainty calculated in Eq. 6 and  $\bar{X}$  was the mean measured value for a specimen. Because  $\bar{X}$  was unique for each specimen, the percent uncertainty varied for each specimen. In Sect. "Measurement uncertainty", we will report the 95% confidence intervals on the uncertainties found for  $T/\theta$ ,  $L$ ,  $K$ , and  $G$ .

**Results**

**Influence of slippage**

The paired t-test between the standard measurement method and the laser measurement method showed that there was no significant difference between the two methods (p-value of 0.2846). As seen in Fig. 5, the medians of the two measurement distributions are virtually identical. Because slipping is not possible when using the laser method, and because there was no difference in data between the laser method and the standard methods, we concluded that slippage was negligible when using the grips approach. As a result, subsequent test results are not differentiated by the method used in measuring rotation.

**Shear modulus distributions for rind and pith tissues**

Rind shear moduli measurements varied from 355 to 1630 MPa and had an approximately normal distribution

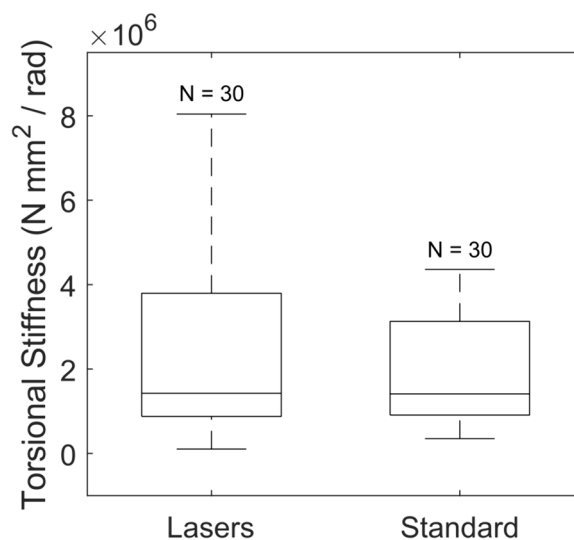


**Fig. 5** torsional stiffness calculated using laser-based angle measurements ("Laser") and the standard MTS method ("Standard")

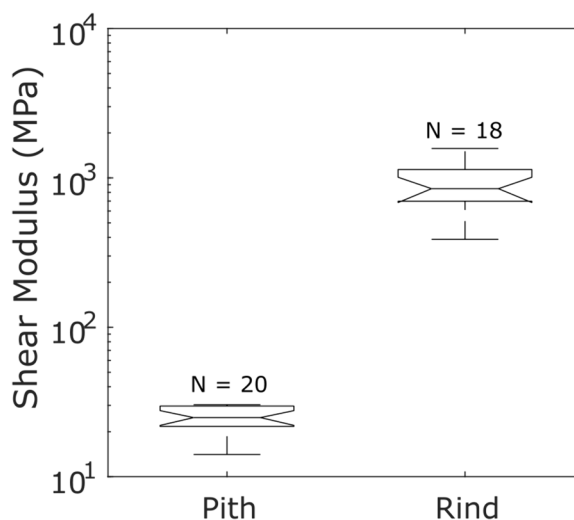


**Fig. 6** Measured pith and rind shear moduli

with a mean of 931 MPa and standard deviation of 334 MPa. Pith shear moduli measurements varied from 13 to 55 MPa and had an approximately normal distribution with a mean of 27 MPa and standard deviation of 10 MPa. The coefficients of variation for these distributions were very similar, 36% for the rind, and 37% for the pith. Figure 6 shows each of these distributions.

**Comparison to similar materials**

Wood and bamboo are relatively similar to maize and can be used as comparison to this study. Moran et al. [12] reported the mean shear modulus of Guadua

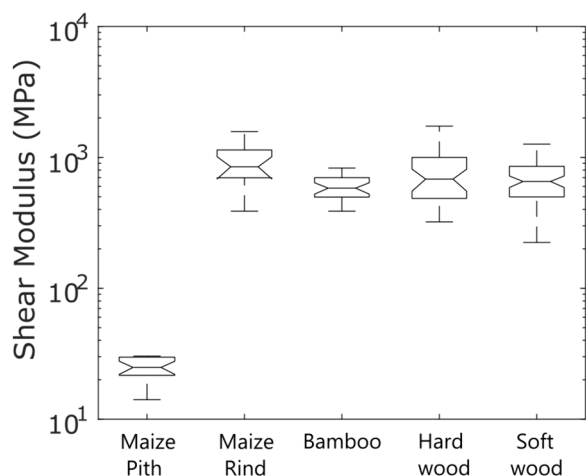


**Fig. 7** Comparison between measured shear modulus values for dry (< 15% moisture) specimens of maize pith, maize rind, bamboo, hardwood and softwood. Bamboo values are from Moran et al. [12], wood values are from Green et al. (1999)

**Table 2** 95% confidence intervals for measurement uncertainties in slope, length, torsional constant, and measurement of shear modulus

	$u_{T/\theta}$	$u_L$	$u_K$	$u_G$
Rind	3.12–4.83%	0.66–0.88%	0.35–0.86%	4.36–12.5%
Pith	4.16–12.8%	0.94–1.17%	0.11–0.16%	3.18–4.75%

Angustifolia (dry) bamboo to be 638 MPa. Green et al. [9] reported the mean shear modulus of hard woods to be 768 MPa, and soft woods to be 692 MPa. Our measured rind shear modulus was found to be slightly higher than these averages, with a mean of 931 MPa.

Figure 7 shows that our measured (dry) rind values fall within both Green and Moran’s ranges for (dry) wood and bamboo. As expected, the measured pith of maize stalks was significantly lower than the other tissues. This is because pith tissue has a density far lower than those materials.

**Measurement uncertainty**

The 95% percent confidence interval of propagated uncertainty for shear modulus was between 5.9% and 13.44% for rind samples. The 95% percent confidence interval of propagated uncertainty for shear modulus was between 5.77% and 7.17% for pith samples. The largest source for this error came from uncertainties in slope ( $u_{T/\theta}$ ). 95% confidence intervals for measurement uncertainties are shown in Table 2.

Because these uncertainties are relatively small, they were not included in the results shown in Fig. 6.

**Discussion**

There are several reasons that we are confident in our measured shear modulus values. Firstly, we are confident that tested specimens did not slip due to applied torque. We know this because t-testing showed that measurement techniques impervious to specimen slipping produced the same results as standard techniques. This means that our data is not biased towards the effects of specimen slipping.

Second, our measured values agree well with reported values for similar materials. Our measured rind modulus fell within the same ranges for wood and bamboo, which are relatively similar to corn tissue. As expected, the measured pith values were much lower than rind values, as has been reported elsewhere for maize tissues [25] (Stubbs et al. 31).

Lastly, our measurement uncertainties in this study were similar to those reported for several methods for measuring the longitudinal stiffness of maize tissues in a prior study [2]. The majority of this error came from variability in repeated specimen testing. Similar phenomena have been seen in previous studies and are common in biological material, so this error is understandable.

**Applications**

The pith and rind shear modulus measured in this study are some of the last influential material properties needed to fully define the material behavior of Ottesen’s parameterized maize stalk models [17]. As shown in Table 1, Poisson’s ratios and transverse shear modulus have also not been measured, but sensitivity analyses have indicated that these properties are less influential in the failure progression of corn stalks [23].

The measurements from this study will be used as material constants in finite element models that are used to predict stalk failure. These models are important in better understanding the phenomenon of stalk lodging, and can be used to decrease stalk lodging through sensitivity and optimization analysis. This study was a necessary step in the development of these models.

**Limitations**

All specimens used in this study came from maize stalks having a relatively low moisture content, (10–15% moisture by weight). An inverse relationship between moisture content and tissue stiffness has been reported in several previous studies of plant tissues [9, 21, 25, 28]. As a result, lower modulus values are to be expected for tissues with higher moisture content.

Several factors such as axial variation, the influence of moisture content, tissue maturity, and other factors were beyond the scope of this study. Axial variation of tissue



bending strength, flexural stiffness, and the influence of the leaf sheath have all been shown to vary along the axial length of the stalk [10, 11, 14]. Shear modulus also likely varies with axial position but was not investigated in this study. Moisture content is known to affect the mechanical properties of maize tissues [25, 29]. In addition, the behavior of immature tissues, diseased tissues, and “goosenecked” stalks have been observed (qualitatively) by the authors to differ significantly from those of mature tissues. As a preliminary study on the longitudinal shear modulus of maize stalk tissues, this study focused on dry tissues and did not investigate the issues of axial variation, tissue maturity, disease, or goosenecking. However, we are hopeful that the measurement methods outlined in this study will be beneficial in supporting future studies that may shed light on the influences of these factors on the shear modulus of maize tissues.

## Conclusions

This study outlines a relatively simple and reliable method for measuring the longitudinal shear modulus of maize rind and pith tissue. The method has relatively low uncertainty and provided the first known estimates for the longitudinal shear modulus of these tissues. The longitudinal shear modulus of the rind was found to be comparable to wood and bamboo with values ranging from 355 to 1630 MPa. The pith tissue values ranged from 13 to 55 MPa. These ranges are important since a full set of measured material properties are required by computational structural models of maize stalks. The results of this research will allow future experimental studies on this property and will enable future computational modeling studies to be based upon solid empirical data instead of “guesstimates”.

## Acknowledgements

This research was supported by the USA National Science Foundation (Award #2046669) and Brigham Young University.

## Author contributions

Carter, J. and Cook, D.D. designed the research. Carter, J., Cook, D.D., and Hoffman, J. wrote the manuscript. Carter, J., Ogilvie, G., and Fjeldsted, B. performed the experimental procedure. All authors read and approved the final manuscript.

## Funding

This study was supported by the National Science Foundation, Arlington, VA, USA (Grant #2046669). The funding agencies did not have any role in designing the study or in collecting, analyzing, interpreting the data or in writing the manuscript.

## Availability of data and materials

The datasets used and/or analyzed during the current study are available from the corresponding author on reasonable request.

## Declarations

### Ethics approval and consent to participate

Not applicable.

### Consent for publication

Not applicable.

### Competing interests

The authors declare that they have no competing interests.

Received: 6 March 2024 Accepted: 30 August 2024

Published online: 30 September 2024

## References

- Al-Zube L, Robertson D, Edwards J, Sun W, Cook D. Measuring the compressive modulus of elasticity of pith-filled plant stems. *Plant Methods*. 2017. <https://doi.org/10.1186/s13007-017-0250-y>.
- Al-Zube L, Wenhuan S, Robertson D, Cook D. The elastic modulus for maize stems. *Plant Methods*. 2018. <https://doi.org/10.1186/s13007-018-0279-6>.
- Askarinejad S, Kotowski P, Rahbar N. Effects of Humidity on shear behavior of bamboo. *Theoret Appl Mech Lett*. 2015. <https://doi.org/10.1016/j.taml.2015.11.007>.
- “ASTM E143–20: Standard Test Method for Shear Modulus at Room Temperature.”
- Boresi AP, Schmidt RJ. *Advanced mechanics of materials*. 6th ed. Hoboken: John Wiley & Sons; 2002.
- Brabec M, Lagana R, Milch J, Tippner J, Sebera V. Utilization of digital image correlation in determining of both longitudinal shear moduli of wood at single torsion test. *Wood Sci Technol*. 2016;51:29–45.
- Budynas R, Sadegh A. *Roark’s formulas for stress and strain*. 9th ed. New York: McGraw Hill; 2020.
- Coleman H, Steele G. *Experimentation, validation, and uncertainty analysis for engineers*. Hoboken: John Wiley & Sons; 2009.
- Senalik CA, Farber B. Chapter 5: Mechanical properties of wood. In: *Wood handbook—wood as an engineering material*. General Technical Report FPL-GTR-282. Madison, WI: U.S. Department of Agriculture, Forest Service, Forest Products Laboratory. 2021;46. <https://research.fs.usda.gov/treesearch/62244>
- Hale J, Webb S, Stubbs C, Cook DD. Assessing axial and temporal effects of the leaf sheath on the flexural stiffness of large-grain stems. *Crop Sci*. 2023;63(2):822–32.
- Martin-Nelson N, Brandon Sutherland M, Yancey CS, Liao CS, Cook DD. Axial variation in flexural stiffness of plant stem segments: measurement methods and the influence of measurement uncertainty. *Plant Methods*. 2021. <https://doi.org/10.1186/s13007-021-00793-8>.
- Moran R, Ghavami K, García J. A new method to measure the axial and shear moduli of bamboo. *Proc Inst Civil Eng Struct Build*. 2017. <https://doi.org/10.1680/jstbu.16.00045>.
- Nelson N, Stubbs CJ, Larson R, Cook DD. Measurement accuracy and uncertainty in plant biomechanics. *J Exp Bot*. 2019;70(14):3649–58.
- Oduntan Y, Kunduru B, Tabaracci K, Mengistie E, McDonald AG, Sekhon RS, Robertson D. The effect of structural bending properties versus material bending properties on maize stalk lodging. *Eur J Agron*. 2024. <https://doi.org/10.1016/j.eja.2024.127262>.
- Ottesen M. *Parametric models of maize stalk morphology*. Masters: Brigham Young University; 2020.
- Ottesen M, Carter J, Hall R, Liu N-W, Cook D. Development and stochastic validation of a parameterized model of maize stalk flexure and buckling. In *Silico Plants*. 2023. <https://doi.org/10.1093/insilicoplants/diad010>.
- Ottesen M, Larson R, Stubbs C, Cook D. A Parameterised model of maize stem cross sectional morphology. *Biosys Eng*. 2022;218:110–23.
- Popov EP, Nagarajan S, Lu ZA. *Mechanics of materials*. 2nd ed. London: Pearson; 2015.
- Chacón RD, Papadopoulos C, Costa FA, Harries KA, Saffar A. “Development of a method to test bamboo culms in direct torsion.” 2022. [https://zenodo.org/records/6975544/files/NOCMAT\\_2022\\_paper\\_103.pdf](https://zenodo.org/records/6975544/files/NOCMAT_2022_paper_103.pdf)
- Robertson D, Julias M, Gardunia B, Barten T, Cook DD. Corn Stalk lodging: a forensic engineering approach provides insights into failure patterns and mechanisms. *Crop Sci*. 2015. <https://doi.org/10.2135/cropsci2015.01.0010>.

21. Rowell R, Skaar C. The chemistry of solid wood; advances in chemistry. Washington, DC: American Chemical Society; 1984.
22. Stubbs C, Baban N, Robertson D, Al-Zube L, Cook D. Bending stress in plant stems: models and assumptions. In: Geitmann A, Gril J, editors. Plant biomechanics. Cham: Springer International Publishing; 2018.
23. Stubbs C, Larson R, Cook D. Maize stalk stiffness and strength are primarily determined by morphological factors. *Sci Rep*. 2022. <https://doi.org/10.1038/s41598-021-04114-w>.
24. Stubbs C, Sun W, Cook D. Measuring the transverse young's modulus of maize rind and pith tissues. *J Biomech*. 2019;84:113–20.
25. Sutherland B, Steele K, Cook D. The Influence of water content on the longitudinal modulus of elasticity of maize stalk tissues. *Plant Methods*. 2022. <https://doi.org/10.1186/s13007-023-01039-5>.
26. USDA. Corn and other feed grains. Washington, DC: USDA; 2023.
27. Von Forell G, Robertson D, Lee SY, Cook DD. Preventing lodging in bioenergy crops: a biomechanical analysis of maize stalks suggests a new approach. *J Exp Bot*. 2015;66(14):4367–71.
28. Zabler S, Paris O, Burgert I, Fratzl P. Moisture changes in the plant cell wall force cellulose crystallites to deform. *J Struct Biol*. 2010;171:133–41.
29. Zhang L, Yang Z, Zhang Q, Guo H. Tensile properties of maize stalk rind. *BioResources*. 2016. <https://doi.org/10.15376/biores.11.3.6151-6161>.
30. Zhang, Lixian, Zhongping Yang, Qiang Zhang, Xinhua Zhu, and Haijun Hu. "Mechanical behavior of corn stalk pith: an experimental and modeling study." 2017.
31. Stubbs CJ, Larson R, Cook DD. Mapping spatially distributed material properties in finite element models of plant tissue using computed tomography. *Biosystems Engineering*. 2020 Dec 1;200:391–9.

### **Publisher's Note**

Springer Nature remains neutral with regard to jurisdictional claims in published maps and institutional affiliations.